Supplement of Atmos. Chem. Phys., 22, 15851–15865, 2022
https://doi.org/10.5194/acp-22-15851-2022-supplement

Atmospheric Chemistry and Physics Open Access

Supplement of

Enhanced natural releases of mercury in response to the reduction in anthropogenic emissions during the COVID-19 lockdown by explainable machine learning

Xiaofei Qin et al.

Correspondence to: Kan Huang (huangkan@fudan.edu.cn) and Congrui Deng (congruideng@fudan.edu.cn)

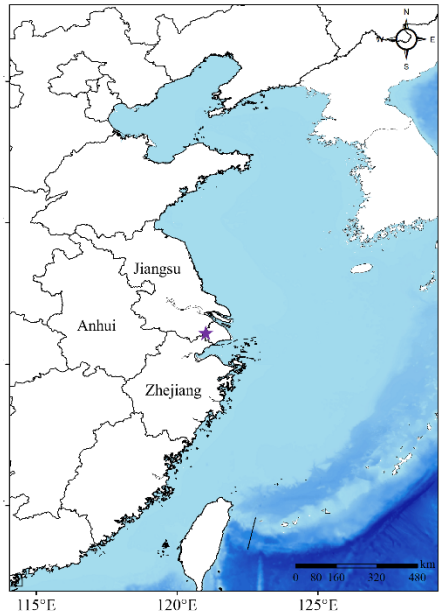

Figure S1. The location of the Dianshan Lake (DSL) site in Shanghai, China (denoted by asterisk in the map)

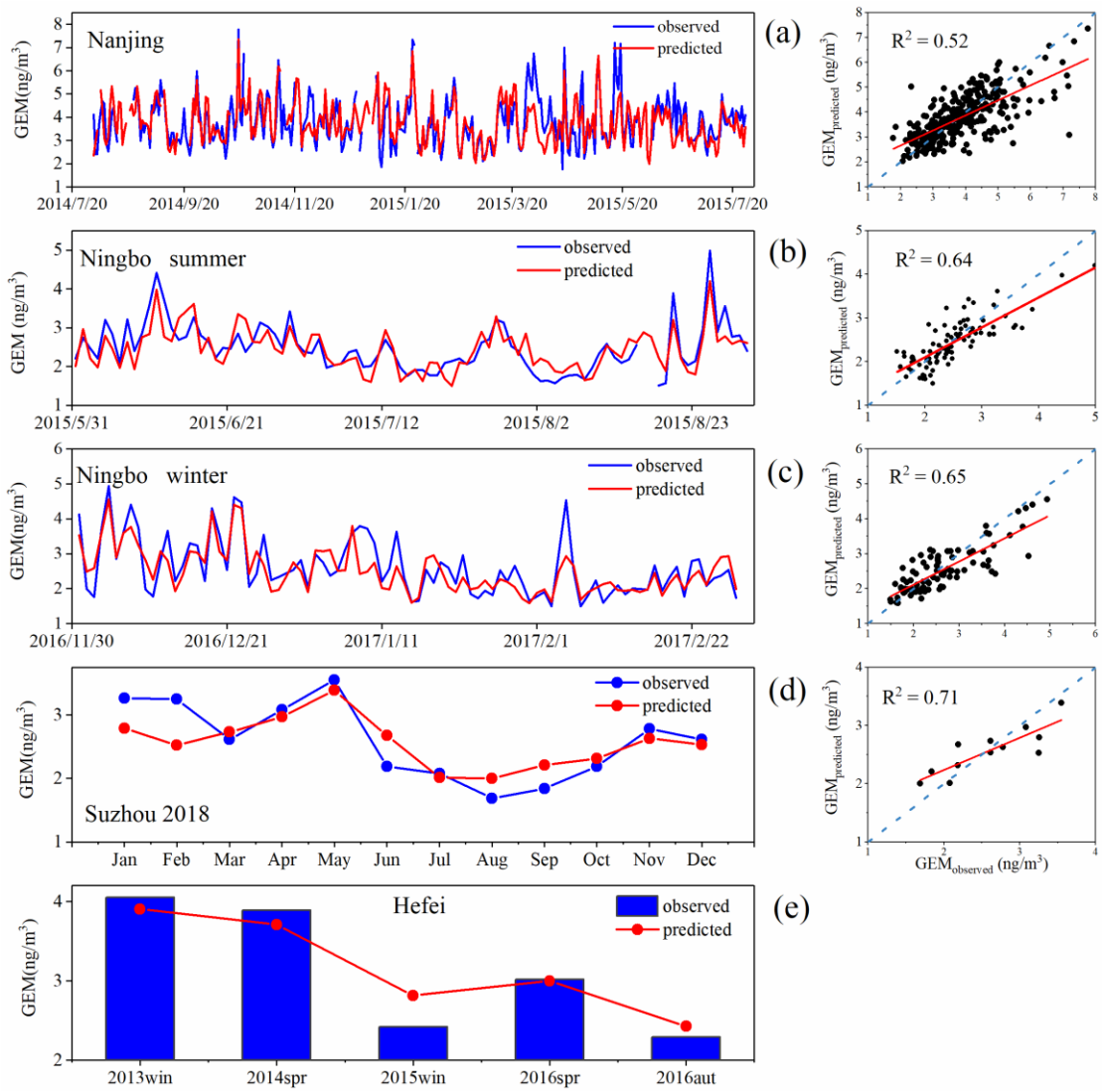

Figure S2. Comparison of observed (blue line) and simulated (red line) GEM concentrations in (a) Nanjing, (b) summer Ningbo, (c) winter Ningbo, (d) Suzhou, and (e) Hefei. The left panel is their time series, and the right panel is their corresponding correlation. The blue dotted line represents the y = x reference line (Qin et al., 2022).

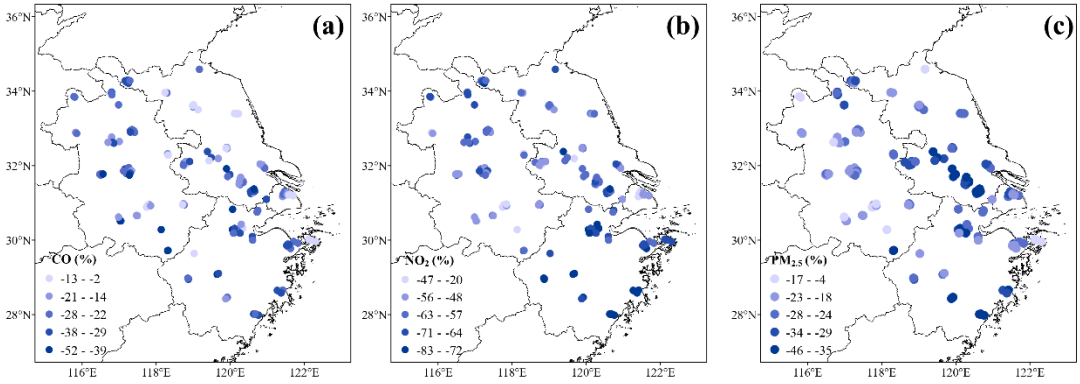

Figure S3. Differences between the average concentrations of (a) CO, (b) NO_2, and (c) $PM_{2.5}$ before and during the COVID-19 lockdown at air quality monitoring stations in the YRD region.

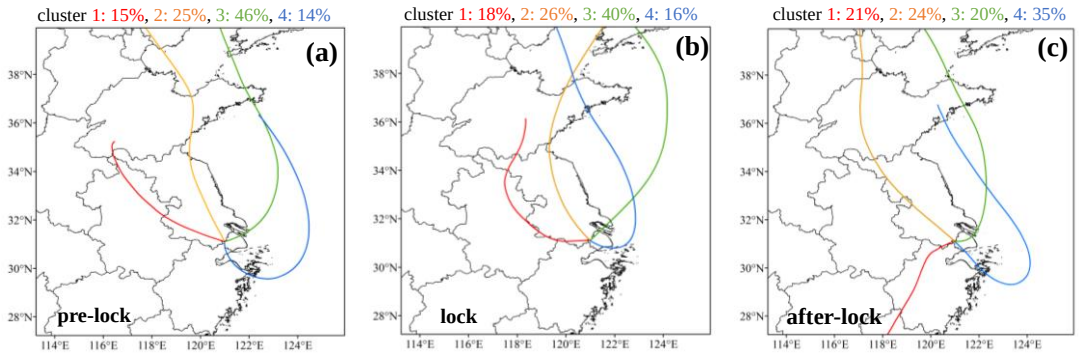

Figure S4. HYSPLIT 3-days backward trajectory cluster analysis at DSL (a) before, (b) during, and (c) after the lockdown.

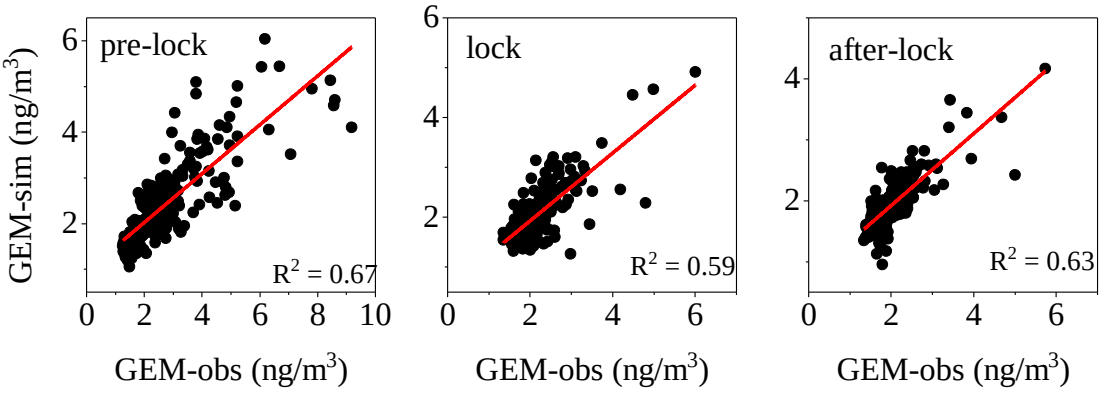

Figure S5. Linear correlation between observed and ANN-simulated GEM concentrations before, during, and after the lockdown.

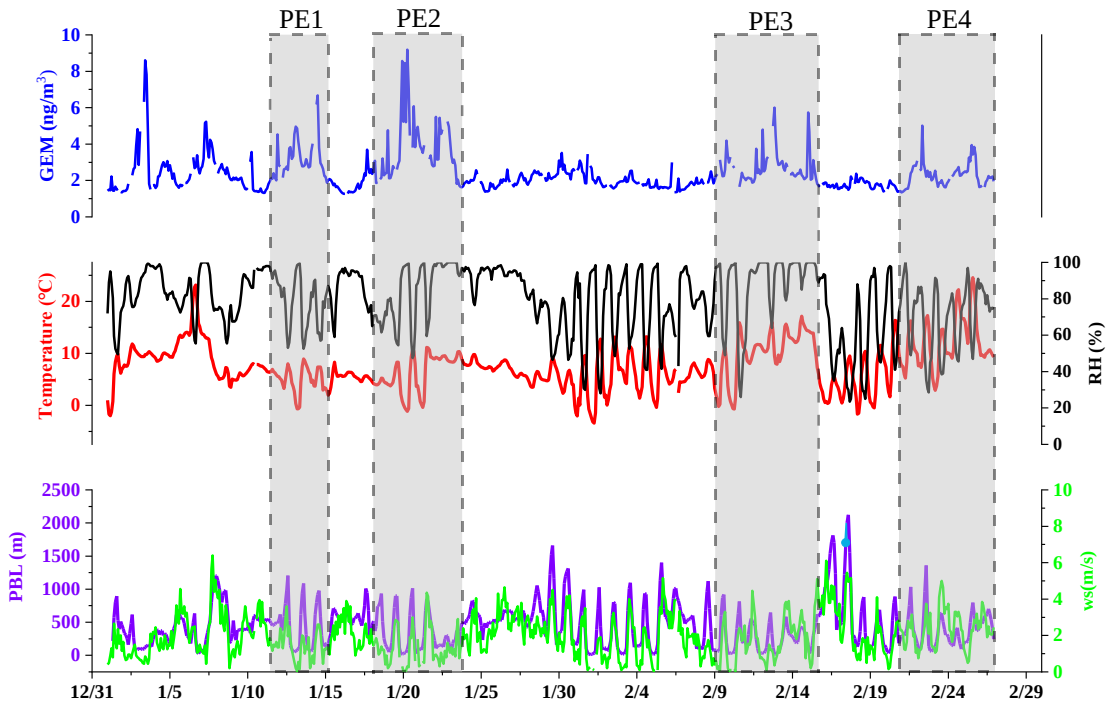

Figure S6. Time series of the observed GEM concentration and meteorological parameters (temperature, relative humidity, PBL height, and wind speed). Four mercury pollution episodes are highlighted by the gray areas.

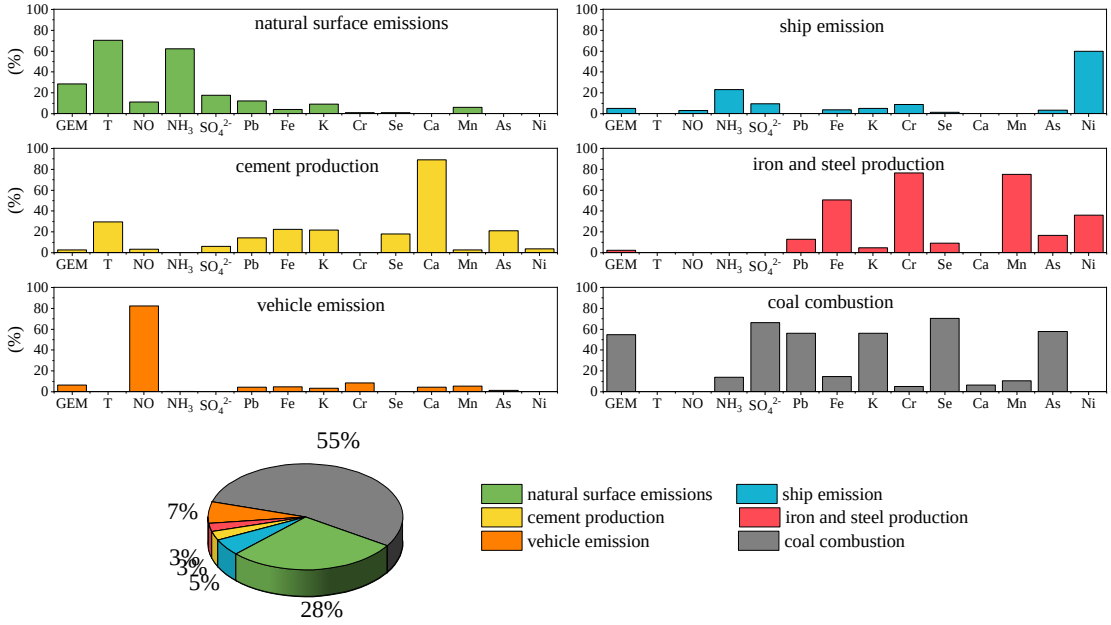

Figure S7. A six - factor source apportionment for GEM based on PMF analysis.

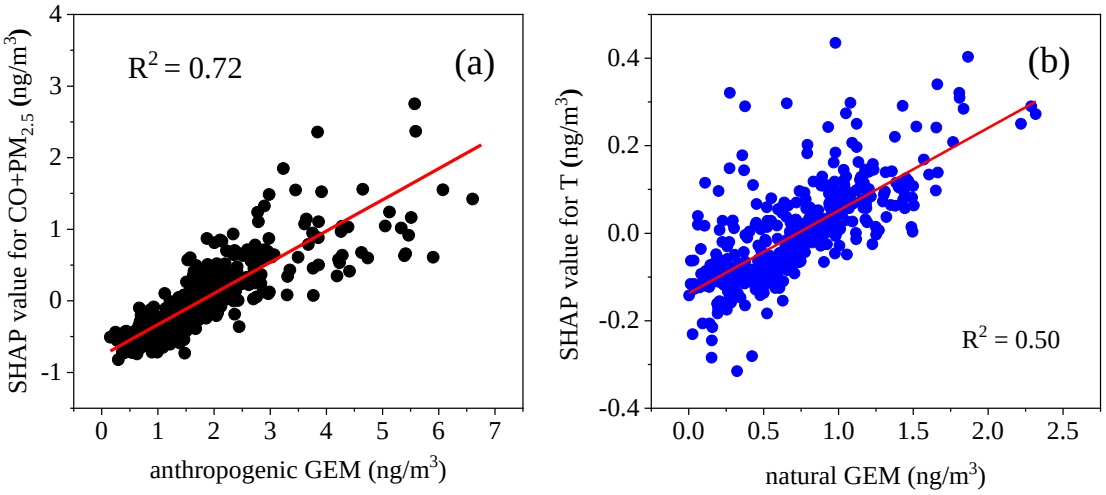

Figure S8. (a) Relationship between the sum of SHAP value for CO and $PM_{2.5}$ with the absolute GEM concentration contributed by anthropogenic sources resolved by PMF model (b) Relationship between SHAP value for temperature with the absolute GEM concentration contributed by natural releases resolved by PMF model

Table S1. Changes in major meteorological factors before, during, and after the lockdown.

	Temperature (℃)	WS(m/s)	RH (%)	PBL(m)	Pressure (Pa)
before	7.2	1.8	83.1	416.6	1024.9
during	6.1	1.9	77.7	483.0	1024.1
after	9.9	2.3	74.4	439.8	1024.5

Table S2. The changes of GEM and the other measured air pollutants before and during the lockdown.

	before	during	relative change (%)
GEM	2.78	2.06	26
SO_2	7.47	6.76	9
NO_2	53.52	23.76	56
CO	0.91	0.61	33
O_3	42.13	83.10	-97
NO	11.53	4.17	64
NO_3^-	23.37	9.73	58
SO_4^{2-}	9.97	7.99	20
NH_4^+	10.88	5.98	45
Ca_2^+	0.14	0.03	77
OC	5.32	4.47	16
EC	2.45	1.52	38
Pb	32.62	21.02	36
Fe	372.22	137.59	63
Cr	5.82	1.06	82
Se	3.37	2.28	32
Ca	67.15	19.86	70
Mn	36.63	9.92	73
As	8.09	5.36	34
Ni	4.02	1.82	55
Zn	112.76	35.26	69
BC	1.87	0.93	51

Note: the units of GEM and all trace elements are ng/m^3. The units of the other air pollutants are $\mu g/m^3$.

Table S3. Summary of Fpeak rotation and comparison of the source profiles and contribution between Base Run and Fpeak Run.

Fpeak strength	dQ (Robust)	%dQ (Robust)	natural surface emissions (%)		ship emission (%)		cement production (%)		iron and steel production (%)		vehicle emission (%)		coal combustion (%)	
			Base run	Fpeak run	Base run	Fpeak run	Base run	Fpeak run	Base run	Fpeak run	Base run	Fpeak run	Base run	Fpeak run
0.5	17	0.12	28.5	27.4	5.1	4.7	2.7	2.3	2.5	2.8	6.5	7.8	54.6	55.0
-0.5	14.8	0.11	28.5	28.3	5.1	5.1	2.7	4.0	2.5	1.9	6.5	6.4	54.6	54.2
1	65	0.47	28.5	26.8	5.1	4.6	2.7	1.6	2.5	3.1	6.5	7.7	54.6	56.1
-1	55.8	0.4	28.5	28.0	5.1	4.6	2.7	5.2	2.5	1.9	6.5	6.4	54.6	53.9

References:

Qin, X., Zhou, S., Li, H., Wang, G., Wang, X., Fu, Q., Duan, Y., Lin, Y., Huo, J., Huang, K., and Deng, C.: Simulation of Spatiotemporal Trends of Gaseous Elemental Mercury in the Yangtze River Delta of Eastern China by an Artificial Neural Network, Environmental Science & Technology Letters, 10.1021/acs.estlett.1c01025, 2022.